cells (*17*) fixed ^{14}C-HCO_3^- into cell carbon (2051 ± 1282 dpm; $n = 3 \pm 1$, mean ± SD) when provided with both sulfide and As(V), whereas no activity occurred with live controls incubated without sulfide (80 ± 69 dpm; $n = 2$) or in a heat-killed control containing both sulfide and As(V) (30 dpm). Strain SLAS-1 was unable to metabolize H_2; however, we have subsequently cultivated enrichments from Searles Lake sediments that use H_2 as an electron donor to support chemolithoautotrophic growth on As(V) (*20*).

Phylogenetic alignment by 16*S* ribosomal RNA (rRNA) gene sequences taxonomically assigned strain SLAS-1 within the order *Halanaerobacteriales* in the Domain Bacteria (Fig. 4). With the exception of the selenate-respiring *Selenihalanaerobacter shriftii* isolated from the Dead Sea (*8*), all other strains are moderate or extremely halophilic, fermentative anaerobes. Strain SLAS-1 was only remotely related to these other species, having the closest sequence similarity to *Halothermothrix orenii* (83.9%) and *Halocella cellulytica* (83.5%). Clearly, strain SLAS-1 is sufficiently genetically distant from these other strains to merit eventual designation as a new species.

Our results show that a full biogeochemical arsenic cycle is operative in the sediments of this salt-encrusted lake, and we have isolated at least one bacterium that can account for some of these observed dynamics. Our demonstration that the abundant As(V) oxyanions present in the brine can be used as a terminal electron acceptor broadens our understanding of the types of processes occurring in such extreme environments, which has implications for possible exobiological life in dense brines (*26*). However, basic research can also aid our interpretation of the interaction of hydrologic and microbial processes affecting arsenic solubility and partitioning in less extreme environments, such as drinking-water aquifers (*27*).

References and Notes

1. B. Javor, *Hypersaline Environments* (Springer, Berlin, 1989).
2. A. Oren, in *Microbiology and Biogeochemistry of Hypersaline Environments*, A. Oren, Ed. (CRC Press, Boca Raton, FL, 1999), pp. 1–12.
3. A. Oren, *Adv. Microb. Ecol.* **10**, 193 (1988).
4. A. Oren, *Microbiol. Mol. Biol. Rev.* **63**, 334 (1999).
5. K. K. Brandt, F. Vester, A. N. Jensen, K. Ingvorsen, *Microb. Ecol.* **41**, 1 (2001).
6. K. B. Sørensen, D. E. Canfield, A. Oren, *Appl. Environ. Microbiol.* **70**, 1608 (2004).
7. M. A. Marvin-DiPasquale, A. Oren, Y. Cohen, R. S. Oremland, *Microbiology and Biogeochemistry of Hypersaline Environments*, A. Oren, Ed. (CRC Press, Boca Raton, FL, 1999), pp. 149–159.
8. J. Switzer Blum, J. F. Stolz, A. Oren, R. S. Oremland, *Arch. Microbiol.* **175**, 208 (2001).
9. R. K. Thauer, K. Jungerman, K. Decker, *Bacteriol. Rev.* **41**, 100 (1977).
10. D. K. Newman, D. Ahmann, F. M. M. Morrell, *Geomicrobiol. J.* **15**, 255 (1998).
11. A. J. Bard, R. Parsons, J. Jordan, *Standard Potentials in Aqueous Solutions* (Dekker, New York, 1985).
12. R. S. Oremland, J. F. Stolz, *Science* **300**, 939 (2003).
13. R. S. Oremland, J. F. Stolz, J. T. Hollibaugh, *FEMS Microbiol. Ecol.* **48**, 15 (2004).
14. R. S. Oremland *et al.*, *Geochim. Cosmochim. Acta* **64**, 3073 (2000).
15. G. I. Smith, *U.S. Geol. Surv. Prof. Pap.* **1043**, 143 (1979).
16. A. R. Felmy, J. H. Weare, *Geochim. Cosmochim. Acta* **50**, 2771 (1986).
17. Materials and methods are available as supporting material on *Science* Online.
18. S. E. Hoeft, T. R. Kulp, J. F. Stolz, J. T. Hollibaugh, R. S. Oremland, *Appl. Environ. Microbiol.* **70**, 2741 (2004).
19. J. T. Hollibaugh *et al.*, *Geochim. Cosmochim. Acta* **69**, 1925 (2005).
20. T. R. Kulp, unpublished data.
21. R. S. Oremland, L. G. Miller, M. J. Whiticar, *Geochim. Cosmochim. Acta* **51**, 2915 (1987).
22. S. E. Hoeft, F. Lucas, J. T. Hollibaugh, R. S. Oremland, *Geomicrobiol. J.* **19**, 1 (2002).
23. R. S. Oremland, S. E. Hoeft, N. Bano, R. A. Hollibaugh, J. T. Hollibaugh, *Appl. Environ. Microbiol.* **68**, 4795 (2002).
24. A. E. Liu, E. Garcia-Dominguez, E. D. Rhine, L. Y. Young, *FEMS Microbiol. Ecol* **48**, 323 (2004).
25. J. Switzer Blum, A. Burns Bindi, J. Buzzelli, J. F. Stolz, R. S. Oremland, *Arch. Microbiol.* **171**, 19 (1998).
26. P. W. J. J. van der Wielen *et al.*, *Science* **307**, 121 (2005).
27. R. S. Oremland, J. F. Stolz, *Trends Microbiol.* **13**, 45 (2005).
28. J. Felsenstein, *Annu. Rev. Genet.* **22**, 521 (1988).

29. We are grateful to D. Hamel, J. Fairchild, C. Hartwig (Searles Valley Minerals Corp., Trona, CA) and to M. Phillips for assistance with access, sampling, and logistics at Searles Lake. We thank H. Dalton, C. Murrell, A. Oren, R. Tabita, and M. Levandowski for constructive criticism of an earlier draft of this manuscript, and H. Cook for initiating our interest in Searles Lake. This work was supported by the U.S. Geological Survey National Research Program and by a grant from NASA's Exobiology Research Program. The GenBank accession number for strain SLAS-1 is AY965613.

Supporting Online Material

www.sciencemag.org/cgi/content/full/308/5726/1305/DC1
SOM Text
Materials and Methods
References

8 February 2005; accepted 22 March 2005
10.1126/science.1110832

Physical Limits and Design Principles for Plant and Fungal Movements

Jan M. Skotheim[1,2] and L. Mahadevan[2,3]*

The typical scales for plant and fungal movements vary over many orders of magnitude in time and length, but they are ultimately based on hydraulics and mechanics. We show that quantification of the length and time scales involved in plant and fungal motions leads to a natural classification, whose physical basis can be understood through an analysis of the mechanics of water transport through an elastic tissue. Our study also suggests a design principle for nonmuscular hydraulically actuated structures: Rapid actuation requires either small size or the enhancement of motion on large scales via elastic instabilities.

From the twirling circumnutation of growing tendrils to the opening and closing of stomata to the growth of fungal hyphae (*1*), plants and fungi are moving all of the time, often too slowly to notice. Rapid movements, though rarer, are used by many plants in essential functions such as seed or sporangium dispersal (Dwarf mistletoe, *Hura crepitans*, and the fungus *Pilobulus*); pollen emplacement (*Catasetum* orchids and *Stylidium* triggerplants); defense (*Mimosa*); and nutrition (Venus flytrap, carnivorous fungi). The mechanisms involved in these movements are varied: *Hura crepitans* (*2*) uses explosive fractures to disperse seeds at speeds as great as 70 m/s, the Venus flytrap (*3*) uses an elastic buckling instability to catch insects in 0.1 s, and the noose-like carnivorous fungus *Dactylaria brochophaga* (*4*) traps nematodes in less than 0.1 s by swelling rapidly.

The diversity of these nonmuscular hydraulic movements, often referred to as nastic movements, raises two related questions: Is there a physical basis for their classification? What, if any, are the principles underlying the biological designs for rapid movements in plants and fungi? To address these, we note that plants and fungi have a common feature that allows us to consider them together here: a cell wall that allows their cells to sustain a large internal (turgor) pressure of up to 10 atmospheres that can be harnessed for growth and motion. Indeed, movements are eventually driven by differential turgor, which may be regulated actively [e.g., by osmotic control as in stomata (*5*)] or passively [e.g., by differential drying as in *Hura crepitans* (*2*)]. In either case, the speed is limited by the rate of fluid transport. Thus, a biophysical charac-

[1]Department of Applied Mathematics and Theoretical Physics, Centre for Mathematical Sciences, University of Cambridge, Cambridge CB3 0WA, UK. [2]Division of Engineering and Applied Sciences, Harvard University, Pierce Hall, 29 Oxford Street, Cambridge, MA 02138, USA. [3]Department of Organismic and Evolutionary Biology, Harvard University Biological Laboratories, 16 Divinity Avenue, Cambridge, MA 02138, USA.

*To whom correspondence should be addressed. E-mail: lm@deas.harvard.edu.

terization of these movements requires knowledge of both the duration of the movement τ and the distance through which the fluid is transported L, which is usually the smallest macroscopic dimension of the moving part. In Fig. 1, we plot τ vs. L and see two categories of movements dominated either by swelling or by elastic instabilities, separated by a dashed line.

To understand this boundary, we recall the physics of water movements through a porous elastic material such as plant tissue. One limit to the speed of movement is determined by the time taken to transport water across the tissue, of characteristic thickness L. Because the fluid and the tissue material are approximately incompressible, the movement of water is compensated by that of the tissue relative to it. Consequently, a flow across a tissue will expand the cells on one side and contract the cells on the other, thereby creating a differential strain. If the typical tissue displacement is denoted by u, the typical fluid velocity field is denoted by v, and the volume fraction of fluid is denoted by φ, the continuity relation embodied in the previous statement reads as $\varphi v = -(1-\varphi)\partial_t u \sim -[(1-\varphi)u]/\tau_p$, where τ_p is the characteristic time for this movement, which is to be determined. Furthermore, the velocity v of the interstitial fluid of viscosity μ in the porous tissue with hydraulic permeability k obeys Darcy's law (*6*), which states that the fluid velocity relative to the medium is proportional to the fluid pressure gradient. Then, if the pressure in the fluid (*7*) p varies over a characteristic length L, we may write $\varphi[v - (u/\tau_p)] \sim kp/\mu L$. This flow is coupled to the tissue elastic stress so that a local balance of forces in the fluid-infiltrated medium yields $Eu/L \sim \varphi p$, where E is the elastic modulus of the tissue (*8*). Substituting the latter expression for the pressure in the expression for the fluid velocity and using the continuity relation written earlier, we find a time scale known as the poroelastic time (*9*, *10*)

$$\tau_p \sim \mu L^2/kE \qquad (1)$$

The poroelastic time characterizes the time for the diffusive equilibration of pressure via fluid transport in soft, wet tissues and is thus of crucial importance in determining the rate of hydraulic actuation in these systems. In Fig. 1, the dotted line corresponds to $\tau_p/L^2 = 1.6$ s/mm^2, consistent with typical values for soft plant tissue (*3*, *11*). This line separates all naturally occurring movements into two categories: slow movements ($\tau > \tau_p$), whose duration is limited by fluid transport; and rapid movements ($\tau < \tau_p$), which rely on elastic instabilities to cross the boundary $\tau = \tau_p$.

The elastic instabilities used by plants and fungi can be divided into two broad categories: snap-buckling and explosive fracture. To sufficiently understand the instability mechanism a particular plant uses requires a detailed study of its geometry [for example (*3*)]. The main difference between these two instabilities is the release mechanism: Snap-buckling involves the rapid geometric changes associated with the buckling of thin shells, whereas explosive fracture involves the rapid geometric changes due to tearing the plant tissue.

The boundary $\tau = \tau_p$ separating the two categories of movement is clearly length-scale dependent and provides a significant barrier for rapid large-scale movements. Elastic instabilities provide the only way to cross the line $\tau = \tau_p$. To illustrate this, we compare *Aldrovanda* (*12*) (circled 1 in Fig. 1) with the closely related Venus flytrap (circled 2 in

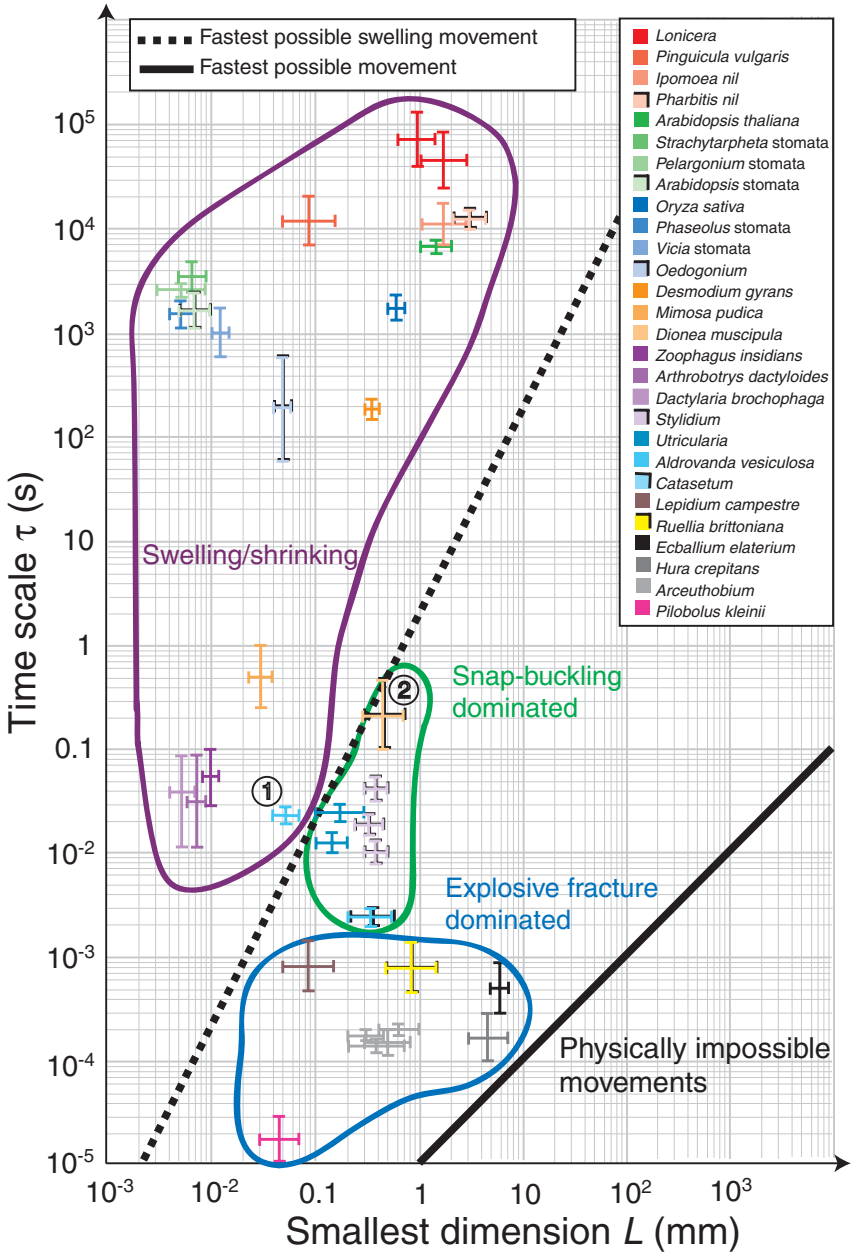

Fig. 1. Classification of plant and fungal movements. The duration of the movement τ is plotted as a function of L, the smallest macroscopic dimension of the moving part (see SOM for detailed references). The dashed line $\tau_p = 1.6\ L^2$ s/mm^2 characterizes the poroelastic time, whereas the solid line $\tau_i = 10^{-5}L$ s/mm characterizes the inertial time. These lines set performance limits on plant and fungal movements while classifying them into two categories: those limited by fluid transport, i.e., $\tau_p < \tau$, and those that use elastic instabilities to go beyond, eventually limited by inertia, i.e., $\tau_i < \tau < \tau_p$. The elastic instabilities can be further categorized as either snap-buckling or explosive fracture. Both types of instabilities rely on geometries capable of gradually storing elastic energy and suddenly releasing it. The difference between the two groups is a matter of how the energy is released: Snap-buckling is associated with a rapid geometric change of a thin shell that does not rupture; explosive fracture involves a rapid geometric change from tissue tearing. The order of the labels in the figure legend coincides with their order in the figure from top to bottom.

Fig. 1), both of which close their leaves rapidly to capture prey; *Aldrovanda* closes its leaves in ~0.02 s, whereas the Venus flytrap closes in ~0.2 s. However, although the leaves of the Venus flytrap snap by reversing their curvature, *Aldrovanda*'s leaves are already initially curved inward so that closure does not produce a snap. To understand how the snapless *Aldrovanda* can be more rapid than the snapping Venus flytrap, we use Eq. (1) for the poroelastic time: for a Venus flytrap leaf of typical thickness $L = 0.5$ mm, $\tau_p = 1.6$ s/mm^2 $(0.5\ \text{mm})^2 \sim 0.4$ s, whereas for an *Aldrovanda* $L = 0.05$ mm, the value of τ_p is ~0.004 s. Because an *Aldrovanda* leaf is about 1/10th the size of the Venus flytrap, it can be actuated 100 times more rapidly and does not require an elastic instability to catch prey, whereas the Venus flytrap does, which is consistent with our classification.

The absolute physical limit of motion in self-actuated mechanical systems is determined by the speed of elastic waves in them, which propagate at a speed that scales as $\sqrt{(E/\rho)}$. This yields an estimate for the inertial time given by

$$\tau_i \sim L\sqrt{(\rho/E)} < \tau \qquad (2)$$

The inertial time scale characterizes the time for wave propagation in mechanical signalling in systems and must be less than τ, the time scale of the motion. In Fig. 1, the solid line denotes $\tau_i/L \sim 10^{-5}$ s/mm, consistent with typical values for soft plant tissue (*3*, *11*), beyond which there can be no natural nastic movements. For the fungus *Pilobolus*'s sporangium discharge (*13*), $L \sim 0.05$ mm, so that $\tau_i \sim 10^{-7}\ \text{s} < 10^{-5}\ \text{s} \sim \tau$, whereas for fruit of *Hura crepitans* (*2*), $L \sim 5$ mm, so that $\tau_i \sim 10^{-5}\ \text{s} < 10^{-4}\ \text{s} \sim \tau$, as shown in Fig. 1. These explosive movements characterize Nature's best attempts to reach the physical limits of autonomous motion in elastic tissues.

In conclusion, we see that the size-dependent inertial-elastic time τ_i and the poroelastic time τ_p given by Eqs. (1) and (2) provide us with a physical basis for the classification of the hydraulic movements in plants and fungi and yield limits on their performance. This implies that the engineering of soft, nonmuscular hydraulically actuated systems for rapid movement requires either small size or the enhancement of motion on large scales via elastic instabilities. Nature has already implemented many such designs exquisitely; we simply need to follow her lead.

References and Notes

1. D. Attenborough, *The Private Life of Plants* (BBC Books, London, 1995).
2. M. D. Swaine, T. Beer, *New Phytol.* **78**, 695 (1977).
3. Y. Forterre, J. M. Skotheim, J. Dumais, L. Mahadevan, *Nature* **433**, 421 (2005).
4. J. Comandon, P. de Fonbrune, *C.R. Soc. Biol. Paris* **129**, 620 (1938).
5. O. V. S. Heath, *New Phytol.* **37**, 385 (1938).
6. This is a reasonable first approximation when the pore size does not change much and when the fluid is Newtonian. Then, the fluid shear viscosity, which characterizes the resistance of the fluid to shear, is a constant. For a simple derivation of Darcy's law in the context of poroelasticity, see (*9*); for a discussion of its implications in confined geometries, see (*10*).
7. The pressure, which has the units of force per unit area, characterizes the local isotropic component of the stress.
8. E is the drained elastic bulk modulus of the tissue, which characterizes the response of the tissue when the fluid is equilibrated. u denotes the typical tissue displacement, i.e., the distance a point in the tissue has moved from its initial position. We have assumed that the material behaves linearly, i.e., that the elastic stress is proportional to the strain. This assumption is usually a good one because the typical strains involved are of the order of a few percent at most.
9. M. A. Biot, *J. Appl. Phys.* **12**, 155 (1941).
10. J. M. Skotheim, L. Mahadevan, *Proc. R. Soc. Lond. A Math. Phys. Eng.* **460**, 1995 (2004).
11. J. French, E. Steudle, *Plant Physiol.* **91**, 719 (1989).
12. J. Ashida, *Mem. Coll. Sci. Kyoto Imp. Univ. B* **IX**, 141 (1934).
13. R. M. Page, *Science* **146**, 925 (1964).

Supporting Online Material

www.sciencemag.org/cgi/content/full/308/5726/1308/DC1
SOM Text
Table S1

29 November 2004; accepted 15 March 2005
10.1126/science.1107976

The Effects of Artificial Selection on the Maize Genome

Stephen I. Wright,[1,3] Irie Vroh Bi,[4]* Steve G. Schroeder,[4] Masanori Yamasaki,[4] John F. Doebley,[5] Michael D. McMullen,[4,6] Brandon S. Gaut[1,2]†

Domestication promotes rapid phenotypic evolution through artificial selection. We investigated the genetic history by which the wild grass teosinte (*Zea mays* ssp. *parviglumis*) was domesticated into modern maize (*Z. mays* ssp. *mays*). Analysis of single-nucleotide polymorphisms in 774 genes indicates that 2 to 4% of these genes experienced artificial selection. The remaining genes retain evidence of a population bottleneck associated with domestication. Candidate selected genes with putative function in plant growth are clustered near quantitative trait loci that contribute to phenotypic differences between maize and teosinte. If we assume that our sample of genes is representative, ~1200 genes throughout the maize genome have been affected by artificial selection.

Maize domestication has resulted in highly modified inflorescence and plant architecture (*1*). Improvement after domestication has also resulted in striking changes in yield, plant habit, biochemical composition, and other traits. At the genetic level, these phenotypic shifts are the result of strong directional (artificial) selection on target genes. With rare exceptions (*2*), targeted genes have not been identified.

Most domesticated plants and animals have experienced a "domestication bottleneck" that reduced genetic diversity relative to their wild ancestor (*3*). This bottleneck affects all genes in the genome and modifies the distribution of genetic variation among loci. The magnitude and variance of the reduction in genetic diversity across loci provide insights into the demographic history of domestication. However, in genes targeted by artificial selection, genetic diversity is reduced above and beyond that caused by the domestication bottleneck (*4*). Selection is similar to a more severe bottleneck (*5*) that removes most (or all) of the genetic variation from a target locus.

Here, we report single-nucleotide polymorphism (SNP) diversity in 774 gene fragments (100 to 900 base pairs) in a sample of 14 maize inbred lines (representing modern maize) and 16 inbred teosintes (tables S1 and S2). In this gene set, we have identified 3463 SNPs in maize and 6136 SNPs in teosinte. The polymorphism data are generally consistent with a population bottleneck during the domestication of maize.

Diversity, as measured by Watterson's estimator of the population mutation parameter θ (*6*), is reduced in maize relative to teosinte (Fig. 1). Our maize sample has about 57% of the variability found in its progenitor. This is somewhat lower than previous estimates that were based on a smaller number of genes (*7*, *8*). The difference in part reflects differences in sampling and the presence of several loci with no polymorphism in maize; 65 maize genes in our data set contain no segregating sites.

[1]Department of Ecology and Evolutionary Biology, [2]Institute of Genomics and Bioinformatics, University of California, Irvine, CA 92697, USA. [3]Department of Biology, York University, Toronto, Ontario M3J 1P3, Canada. [4]Department of Agronomy, Plant Science Unit, University of Missouri, Columbia, MO 65211, USA. [5]Department of Genetics, University of Wisconsin, Madison, WI 53706, USA. [6]Plant Genetics Research Unit, USDA–Agricultural Research Service, Columbia, MO 65211, USA.

*Present address: Institute for Genomic Diversity, Cornell University, Ithaca, NY 14853, USA.
†To whom correspondence should be addressed. E-mail: bgaut@uci.edu